Supplementary Information

Single stereocenter inversion of a cyclic tetrapeptide enables the detoxification of lead-exposed mice

Tagwa A. Mohammed, Luca Sauser, Erica Pedron, Yaël A. Hodel, Tadeáš Kalvoda, Francesco Prisco, Lubomír Rulíšek, Jason P. Holland,* and Michal S. Shoshan*

Table of Contents

Safety statement

No unexpected or unusually high safety hazards were encountered during the described procedures.

1 General protocols for peptide synthesis

1.1 Coupling of the first amino acid (AA)

The CTC resin was washed with dry CH_2Cl_2, and a mixture of Fmoc-Xaa-OH (3 equiv.) and Hünig's base (6 equiv.) in dry CH_2Cl_2 was added. The resin was agitated for 2 h and then washed with DMF (3x) and CH_2Cl_2 (3x).

1.2 Fmoc deprotection

A 20% piperidine solution in DMF was added to the resin, and the suspension was agitated for 10 min. The procedure was conducted twice. The resin was then washed with DMF (3x) and CH_2Cl_2 (3x).

1.3 Peptide couplings

Fmoc-Xaa-OH (3 equiv.) and HATU (2.7 equiv.) were dissolved in DMF (0.8 M), and Hünig's base (6 equiv.) was added. After 1 minute, the mixture was added to the amino-functionalized resin that was suspended in a minimal amount of DMF. The mixture was agitated for 60 min and washed with DMF (3x) and CH_2Cl_2 (3x). Couplings were monitored by test cleavage of a small portion of resin and subsequent LCMS analysis.

1.4 Cleavage of the side-chain protected peptides from the solid support

The resin was agitated six times for 5 min in 1% TFA in CH_2Cl_2, and the solution was collected by filtration. The filtrate was concentrated under reduced pressure, and the product was precipitated from cold Et_2O. The white solid was isolated by centrifugation of the suspension and decanting the supernatant. The solid was triturated with Et_2O twice, and the residual white solid was dried under a stream of nitrogen. It was then suspended in CH_3CN:H_2O (1:1), and lyophilized to obtain the peptide as a white solid.

1.5 Head-to-tail cyclization of the peptides

To a backboned deprotected and side-chain protected peptide (0.2 mmol) in CH_2Cl_2 (1 L), PyBOP (0.3 mmol) and Hünig's base (0.6 mmol) were added. The reaction was

agitated at rt for 16-72 h until full conversion was detected by LCMS. The solvent was removed under reduced pressure, and the product was precipitated with H_2O. The white solid was isolated by centrifugation of the suspension and decanting the supernatant. The solid was triturated twice with H_2O, and the residual white solid was suspended in a mixture of CH_3CN:H_2O (1:1) and lyophilized to obtain the peptide as a white solid.

1.6 Side-chain deprotection of cyclic peptides

The peptide was agitated for up to 2 h in a mixture of TFA:H_2O:TIPS:EDT (87.5:2.5:2.5:7.5). The solution was concentrated under a stream of nitrogen, and the product was precipitated from cold Et_2O. The white solid was isolated by centrifugation of the suspension and decanting the supernatant. The solid was triturated with Et_2O twice, and the residual white solid was dried under a stream of nitrogen. It was then dissolved in H_2O and lyophilized to obtain the peptide as a white solid.

1.7 Peptide purification

20 mL of CH_3CN were added to the deprotected cyclized peptide. The solid peptide was isolated by centrifugation of the suspension and decanting the supernatant. The solid was triturated with CH_3CN (x3). The residual white solid was dried under a stream of nitrogen, dissolved in CH_3CN:H_2O (1:1), and lyophilized to obtain the cyclic tetrapeptide as a white solid.

1.8 Ion exchange and desalting

The peptide was isolated as a TFA salt after cleavage from the resin and purification. The peptide (~100 mg) was reacted with HCl (1 M, ~1 mL) for 1 min, and the solvent was removed under reduced pressure. The procedure was repeated at least two more times until no TFA signal was observed, as indicated by recording ^{19}F NMR spectra.

2 Synthesis and analytical data of the peptides

2.1 cyc-[(Cys-βAsp)$_2$] (**2**)

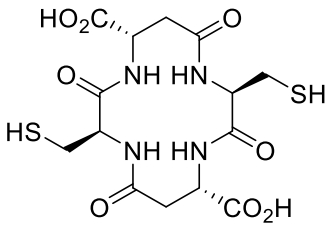

Peptide cyclization was complete after 48 h, yielding 39%.

^{1}H NMR (400 MHz, DMSO-*d*$_6$) δ (ppm) 8.60 (d, *J* = 7.7 Hz, 2H), 7.49 (d, *J* = 8.4 Hz, 2H), 4.49 (quint, *J* = 4.1 Hz, 2H), 4.23 (q, *J* = 7.4 Hz, 2H), 2.89-2.78 (m, 4H), 2.60-2.52 (m, 4H), 2.37 (t, *J* = 8.6 Hz, 2H)

^{13}C{^{1}H} NMR (101 MHz, DMSO-*d*$_6$) δ (ppm) 172.0, 170.0, 169.3, 54.8, 47.9, 36.1, 22.6

HR-MS-ESI *m/z*: calculated for $C_{14}H_{19}N_4O_8S_2^-$ [M-H]$^-$ 435.06498; found: 435.06564

2.2 cyc-[Cys-βAsp-Cys-βAla] (**3**)

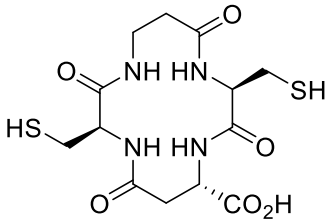

Peptide cyclization was complete after 72 h, yielding 40%.

^{1}H NMR (400 MHz, D$_2$O) δ (ppm) 4.39 (t, *J* = 4.6 Hz, 1H), 4.31 (t, *J* = 7.3 Hz, 1H), 4.15 (dd, *J* = 5.9, 6.9 Hz, 1H), 3.59-3.52 (m, 1H), 3.42-3.36 (m, 1H), 3.02 (dd, *J* = 4.1, 16.1 Hz, 1H), 2.94 (d, *J* = 5.2 Hz, 1H), 2.91-2.82 (m, 2H), 2.74-2.68 (m, 2H), 2.66-2.61 (m, 1H) 2.55-2.49 (m, 1H)

^{13}C{^{1}H} NMR (101 MHz, D$_2$O) δ (ppm) 177.0, 174.5, 172.9, 172.2, 168.4, 58.5, 58.0, 50.8, 36.7, 35.6, 33.9, 25.8, 24.5

HR-MS-ESI *m/z*: calculated for $C_{13}H_{19}N_4O_6S_2^-$ [M-H]$^-$ 391.07515; found: 391.07519

2.3 cyc-[Cys-βAsp-Cys-βDAsp] (**4**)

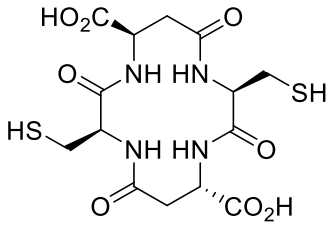

Peptide cyclization was complete after 72 h, yielding 53%.

^{1}H NMR (400 MHz, D_2O) δ (ppm) 4.47 (dd, *J* = 3.1, 4.7 Hz, 1H), 4.39 (dd, *J* = 4.1, 10.4 Hz, 1H), 4.22 (t, *J* = 7.2 Hz, 1H) 3.96 (t, *J* = 6.4 Hz, 1H), 2.88 (dd, *J* = 2.9, 16.6 Hz, 1H), 2.70-2.58 (m, 6H), 2.55-2.47 (m, 1H), 1.04-1.00 (m, 2H)

^{13}C{^{1}H} NMR (101 MHz, D_2O) δ (ppm) 176.6, 176.3, 172.6, 172.2, 171.9, 170.8, 56.9, 55.5, 51.7, 50.1, 36.6, 36.2, 24.5, 23.1

HR-MS-ESI *m/z*: calculated for $C_{14}H_{19}N_4O_8S_2^-$ $[M-H]^-$ 435.06498; found: 435.06482

3 *In vitro* cell viability studies

3.1 Sample preparation

DMSA was purchased in its neutral form, which is insoluble in H_2O. It was dissolved in the presence of 2 equiv. NaOH, similarly to the formulation in the clinic. (1)

Peptides (18 μmol) were freshly dissolved in a NaOH solution (240 mM, 150 μL) to achieve a final Na_2(peptide) concentration of 120 mM. The peptide solutions were used immediately for biological assays.

3.2 Recovery and rescue assay

HT-29 cells were chosen as a representative human cell line due to their sensitivity to Pb, and as their medium, RPMI-1640, is compatible with Pb(II) ions, thereby inhibiting metal precipitation.

HT-29 cells were grown in 25 mM HEPES RPMI-1640 medium, supplemented with 1% L-glutamine, 1% penicillin/streptomycin, and 10% FCS (standardized) at 37 °C and 5% CO_2. 96-well plates were prepared so that each well contained 10,000 cells in 100 μL of medium, and the cells were allowed to adhere overnight.

To all wells except the positive control ones, 10 μL of 22 mM $Pb(NO_3)_2$ was added (final concentration 2 mM). 10 μL of H_2O was added to the positive control wells. 60 min after the addition of the metal salt, 10 μL of each solution of the examined CA (2.4, 6, 12, 24, and 48 mM) were added to reach final concentrations of 0.2, 0.5, 1, 2, and 4 mM (which are 0.1, 0.25, 0.5, 1, 2, and 4 equivalents, respectively). To the positive control wells containing no metal and the negative control wells containing metal but no CAs, 10 μL of H_2O were added. Each condition was performed in triplicate.

The plates were incubated at 37 °C, and 5% CO_2 for an additional 23 h, after which the medium was removed, the wells were washed with H_2O, and 50 μL of CV solution (2, 3) (500 mg CV powder in 20 mL CH_3OH and 80 mL H_2O) were added to each well. The plates were gently shaken (50 rpm) for 20 min. The plates were then washed with H_2O until no more unbound dye was visible, and they were allowed to dry overnight. 100 μL of CH_3OH was added to each well, and the plates were gently shaken (50 rpm) for 20 min, after which their absorbance at 560 nm was recorded.

The recovery value of each concentration of a peptide was calculated according to Equation S1 (relative to the negative control):

$$Recovery\% = \frac{A[CA_X] - A[blank]}{A[NEG] - A[blank]} \times 100\%$$

A[CA$_X$] – absorbance of the pre-toxified well in the presence of X mM of CA

A[blank] – absorbance of an empty well

A[NEG] – absorbance of the pre-toxified well that was not treated with any CA

Each experiment was performed in three independent repeats. Values are mean ± SD.

The rescue value of each concentration of a peptide was calculated according to Equation S2 (relative to the positive control):

$$Rescue\% = \frac{A[CA_X] - A[blank]}{A[POS] - A[blank]} \times 100\%$$

A[CA$_X$] – absorbance of the pre-toxified well in the presence of X mM of CA

A[blank] – absorbance of an empty well

A[POS] – absorbance of the well where Pb(II) was not added to it, and that was not treated with any CA

Each experiment was performed in three independent repeats. Values are mean ± SD.

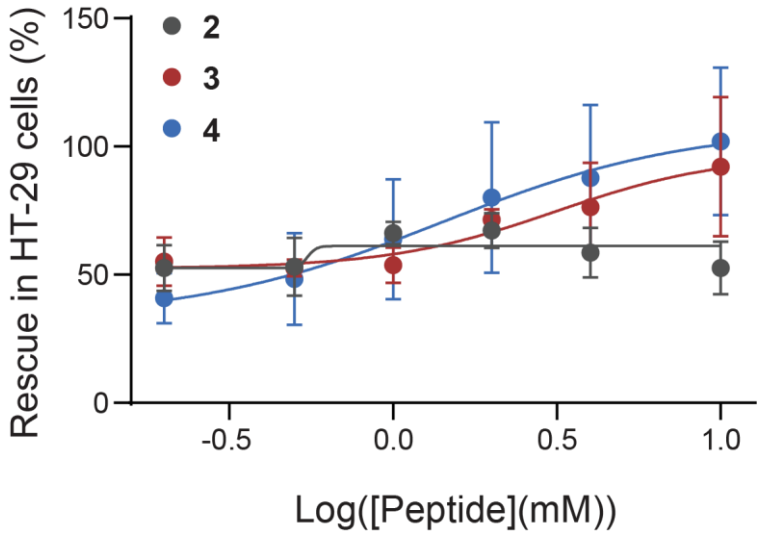

Figure S1 Dose-dependent rescue of HT-29 cells treated with $Pb(NO_3)_2$ (2 mM) followed by the administration of cyclic peptides **2**, **3**, or **4** (as di-Na salts; 1 h after the addition of Pb(II) ions). Values are calculated relative to normal as the positive control.

3.3 Toxicity assay

96-well plates were prepared such that every well contained 10,000 HT-29 cells in 100 µL medium, and the cells were allowed to adhere overnight.

To all wells but the positive control wells, 10 µL of each solution of the examined CAs (2.4, 6, 12, 24, and 48 mM) was added to reach final concentrations of 0.2, 0.5, 1, 2, and 4 mM. To the positive control wells, 10 µL of H_2O was added. Each condition was performed in triplicate. The plates were incubated at 37 °C, and 5% CO_2 for 23 h, after which the medium was removed, the wells were washed with fresh medium, and 50 µL of CV solution (2) (500 mg CV powder in 20 mL CH_3OH and 80 mL H_2O) was added to each well. The plates were gently shaken (50 rpm) for 20 min. The plates were then washed with H_2O until no more unbound dye was visible, and they were allowed to dry overnight. 100 µL of CH_3OH was added to each well, and the plates were gently shaken (50 rpm) for 20 min, after which their absorbance at 560 nm was recorded.

The toxicity of each concentration of a CA was calculated according to Equation S3:

$$Toxicity\% = \frac{A[CA_X] - A[blank]}{A[POS] - A[blank]} \times 100\%$$

$A[CA_X]$ – absorbance of well in the presence of X mM of CA

A[blank] – absorbance of an empty well

A[POS] – absorbance of a well that contains no CAs

Each experiment was performed in three independent repeats. Values are mean ± SD.

4 Complexes characterization

4.1 Affinity and stoichiometry determination with $Pb(NO_3)_2$, $ZnCl_2$ or $CaCl_2$ by ITC

Titrations were performed in 20 mM Tris buffer, pH 6.5, at 25 °C, with the metal salt solution (280 µL) titrated into the peptide solution (1.8 mL) at the concentrations listed in Table S1.

Table S1 Peptides and metal salt solutions concentrations for ITC-monitored titrations

	[Peptide] (µM)	Salt	[Salt] (mM)
2	100	$Pb(NO_3)_2$	3.0
4	200	$Pb(NO_3)_2$	0.6
4	200	$ZnCl_2$	3.0
4	200	$CaCl_2$	5.0

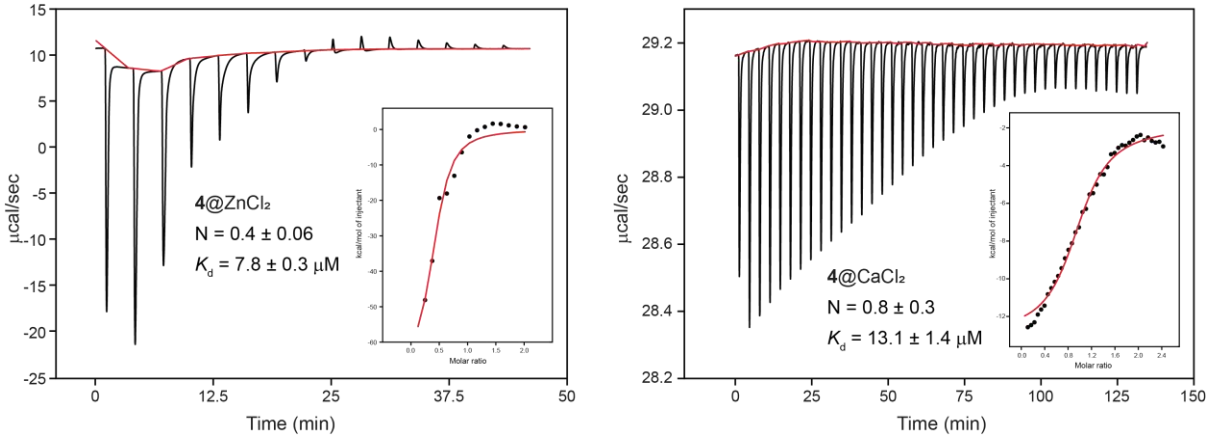

Figure S2 ITC raw and integrated data for the titration of peptide **4** with Zn(II) (left) or Ca(II) (right) ions. Titrations were performed at 25 °C in 20 mM Tris buffer at pH 6.5.

4.2 UV-Vis titration of $Pb(NO_3)_2$ with peptides

To aliquots of peptide (25 μM) in 20 mM Tris buffer pH 6.5, $Pb(NO_3)_2$ was added at final concentrations of 7.25-125 μM (equal to 0.25-5 equiv.), and the total volume was adjusted to 200 μL with Tris buffer. The spectra of each solution were recorded (200-400 nm), and a blank spectrum of only the buffer was omitted from all spectra.

4.3 Determination of Pb-peptide complexes stability by UV-Vis titrations

To aliquots of peptide and $Pb(NO_3)_2$ at final concentrations of 25 and 50 μM, respectively, in 20 mM Tris buffer pH 6.5, $ZnCl_2$ (4 mM) or $CaCl_2$ (40 mM) were added in 1-10 equivalents for $ZnCl_2$ or 10-100 equivalents for $CaCl_2$ compared with the peptide's concentration. The total volume was brought to 200 μL with Tris buffer. The spectra of each solution were recorded (200-400 nm), and a blank spectrum of only the buffer was omitted from all spectra.

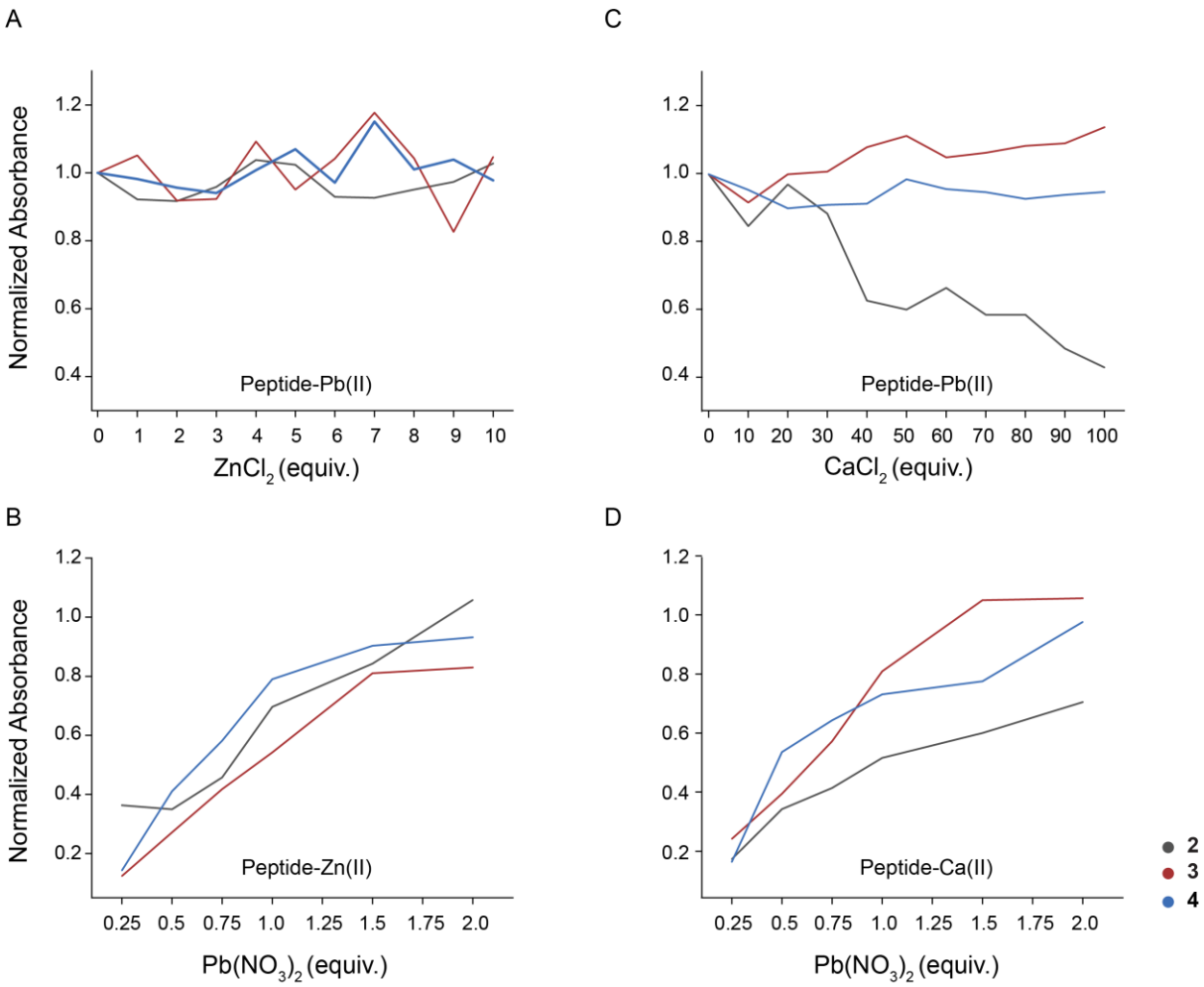
A
Normalized Absorbance
1.2
1.0
0.8
0.6
0.4
Peptide-Pb(II)
0 1 2 3 4 5 6 7 8 9 10
ZnCl2 (equiv.)
C
1.2
1.0
0.8
0.6
0.4
Peptide-Pb(II)
0 10 20 30 40 50 60 70 80 90 100
CaCl2 (equiv.)
B
Normalized Absorbance
1.2
1.0
0.8
0.6
0.4
0.2
Peptide-Zn(II)
0.25 0.5 0.75 1.0 1.25 1.5 1.75 2.0
Pb(NO3)2 (equiv.)
D
1.2
1.0
0.8
0.6
0.4
0.2
Peptide-Ca(II)
0.25 0.5 0.75 1.0 1.25 1.5 1.75 2.0
Pb(NO3)2 (equiv.)
2
3
4

Figure S3 (A) UV-monitored competitor-titrations of Pb-peptide complexes (25 μM for peptides and 50 μM $Pb(NO_3)_2$) with $ZnCl_2$ (0-250 μM; 0-10 equiv. to peptide's concentration). (B) UV-monitored titration of $Pb(NO_3)_2$ (0-50 μM; 0-2 equiv.) to mixtures of peptides and $ZnCl_2$ (25 μM and 250 μM, respectively). (C) UV-monitored competitor-titrations of Pb-peptide complexes (25 μM for peptides and 50 μM $Pb(NO_3)_2$) with $CaCl_2$ (0-2.5 mM; 0-100 equiv. to Pb(II) ions; the same graph is also presented in Figure 2C). (D) UV-monitored titration of $Pb(NO_3)_2$ (0-50 μM; 0-2 equiv.) to mixtures of peptides and $CaCl_2$ (25 μM and 2.5 mM, respectively).

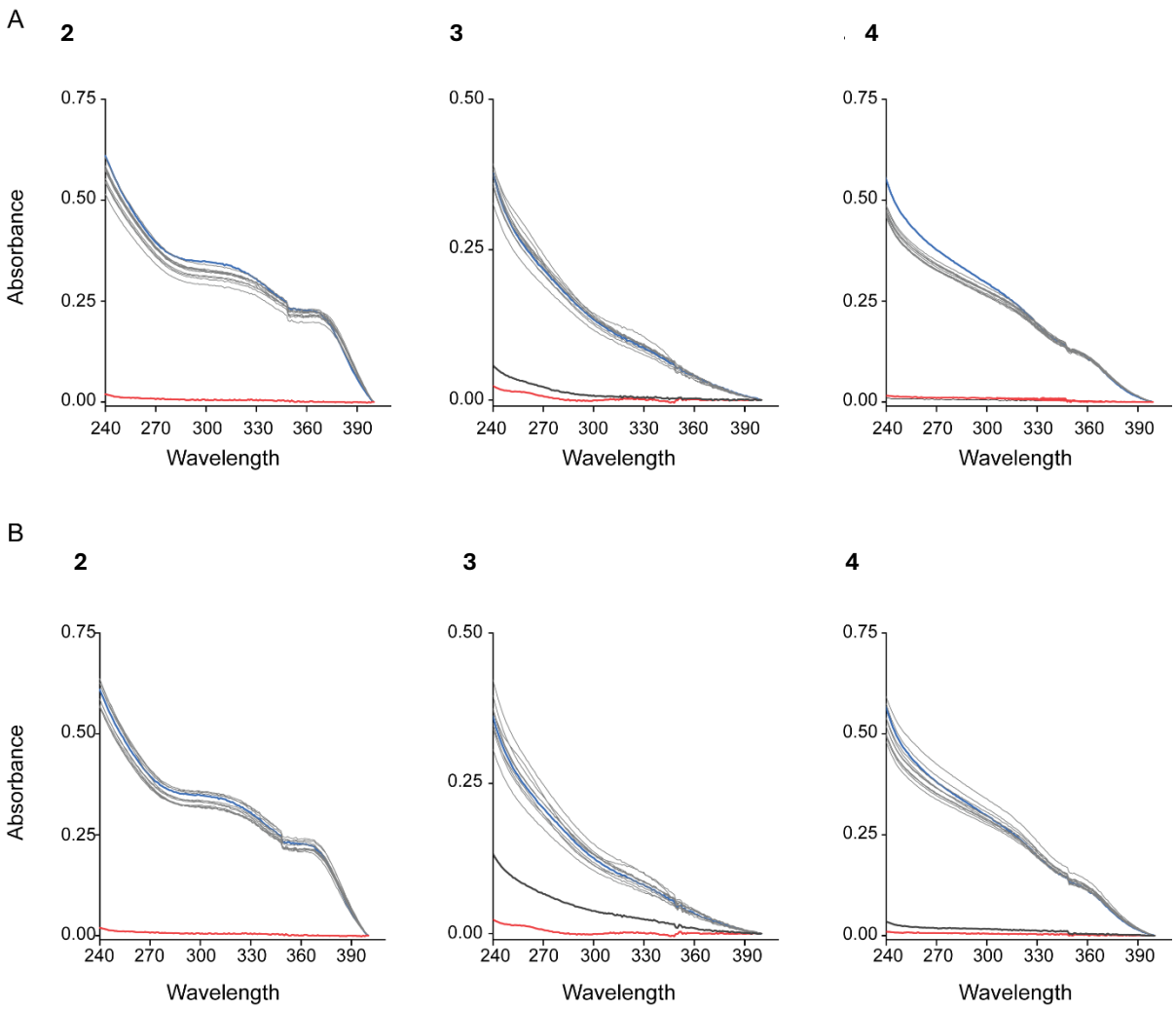

Figure S4 (A) UV-monitored back-titrations of peptides-Pb(II) complexes (25 μM) with $CaCl_2$ (0-100 equiv., compared to the peptide's concentration), where red spectra are for *apo* peptides, black spectra are for peptides with only $CaCl_2$ (100 equiv.), and blue spectra are for peptides with only $Pb(NO_3)_2$ (2 equiv.), (B) UV-monitored back-titrations of peptides-Pb(II) complexes (25 μM) with $ZnCl_2$ (0-10 equiv., compared to the peptide's concentration), where red spectra are for *apo* peptides, black spectra are for peptides with only $ZnCl_2$ (10 equiv.), and blue spectra are for peptides with only $Pb(NO_3)_2$ (2 equiv.).

4.4 Determination of peptide selectivity by UV-Vis titrations

To aliquots of peptides (25 µM) and $CaCl_2$ (2.5 mM) or $ZnCl_2$ (250 µM) in 20 mM Tris buffer, pH 6.5, $Pb(NO_3)_2$ was added after 1 h in 0.25 - 2 equivalents compared with the concentration of the peptide (25 µM), and the total volume was brought to 200 µL with Tris buffer. The spectra of each solution were recorded (200-400 nm), and the blank spectrum of only the buffer was omitted from all spectra.

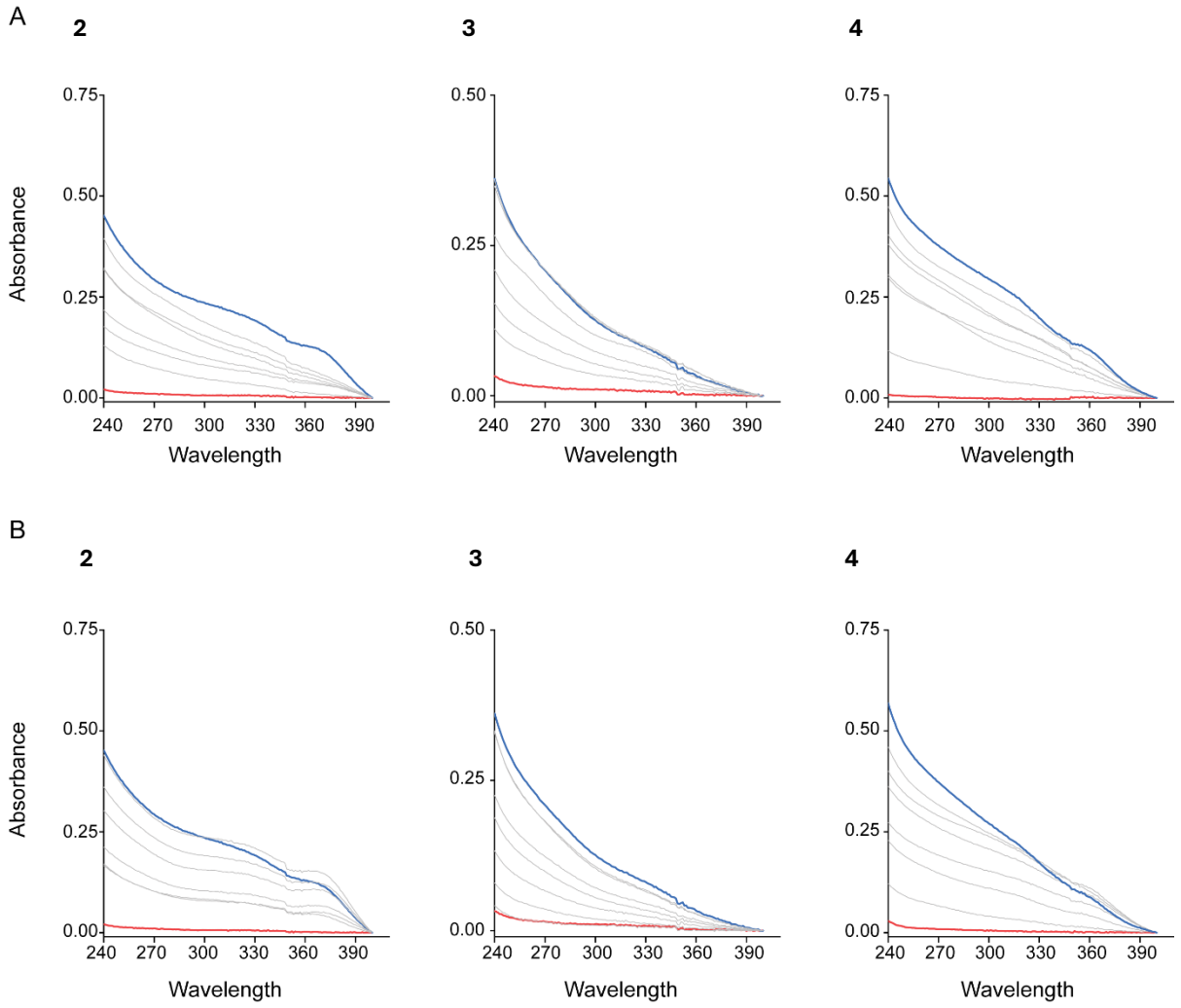

Figure S5 (A) UV-monitored titrations of peptides (25 µM) and $CaCl_2$ (2.5 mM) with $Pb(NO_3)_2$ (0.25-2 equiv.), where red spectra are for *apo* peptides, and blue spectra are for peptides with only $Pb(NO_3)_2$ (2 equiv.). (B) UV-monitored titrations of peptides (25 µM) and $ZnCl_2$ (250 µM) with $Pb(NO_3)_2$ (0.25-2 equiv.), where red spectra are for *apo* peptides, and blue spectra are for peptides with only $Pb(NO_3)_2$ (2 equiv.).

5 Peptides stability against oxidation

To shed light on the stability of these peptides during the time frame of the *in vitro* and *in vivo* assays, we evaluated their oxidation rate, utilizing Ellman's test. As all three peptides have two thiols, the possibility of them forming an intramolecular disulfide bridge is high. We therefore dissolved the peptides in H_2O at pH 8 in the presence of Tris buffer. Then we added the Ellman's reagent at different time intervals to determine the percentage of the reduced peptide. We observed that even after 24 h, more than 80% of peptides **2** and **4**, and over 60% of peptide **3**, remain reduced (Figure S6). We conclude that the second carboxylic acid, present in peptides **2** and **4**, significantly reduces the oxidation rate, either through an electronic effect or steric hindrance.

Calibration curve: to a 96-well plate with freshly-prepared solutions of Ac-Cys-OMe (25-200 μM) in H_2O supplemented with 10% 1 M Tris buffer pH 8.0, a fresh solution of Ellman's reagent (DTNB; final concentration of 300 μM in H_2O supplemented with 12.5 mM NaOAc) was added. (4) The absorbance of each well at 412 nm was then determined, and the average and standard deviation across six wells containing the same AA concentration were calculated and linearly plotted in Origin.

Eight 96-well plates were prepared identically with fresh solutions of peptides **2**-**4** (100 μM) in H_2O supplemented with 10% 1 M Tris buffer, pH 8.0, with each condition replicated in 6 wells. A fresh solution of Ellman's reagent (DTNB; final concentration of 300 μM in H_2O supplemented with 12.5 mM NaOAc) was added at different intervals: t = 0, 0.5, 1, 2, 4, 6, 8, 12 h.(4) The absorbance of each well at 412 nm was then determined, and the concentration of free thiol per well was calculated according to the calibration curve. For each time frame, the average and standard deviation were calculated. The percentage of the reduced peptide was calculated according to Equation S4:

$$Reduced\ peptide\% = \frac{A[peptide\ t = x] - A[blank]}{A[peptide\ t = 0] - A[blank]} \times 100\%$$

[peptide t=x] – concentration of the peptide solution at t = x (x > 0)

[peptide t=0] – concentration of the peptide solution at t = 0

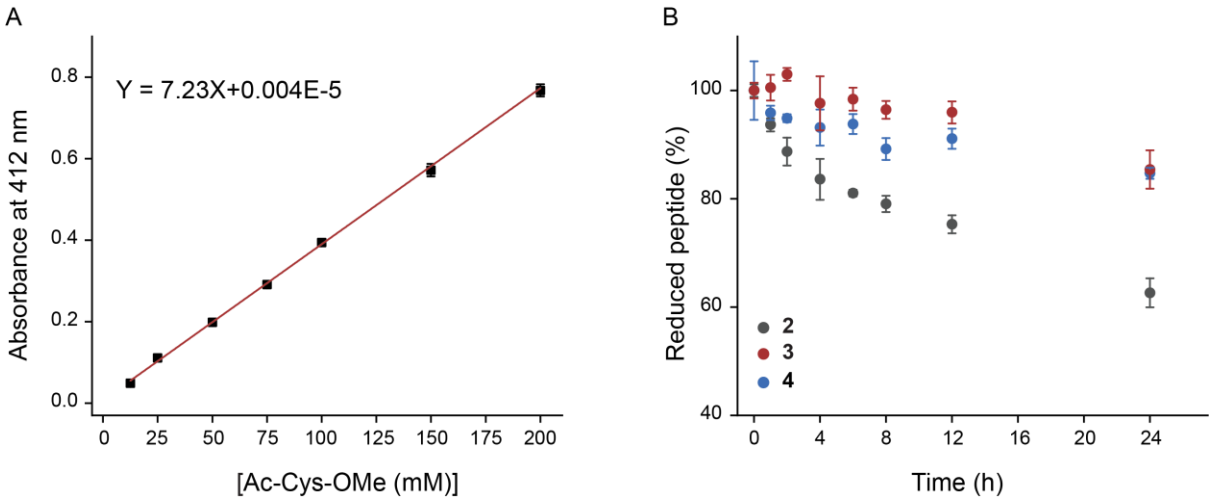

Figure S6 (A) Calibration curve of Ac-Cys-OMe at various concentrations in pH 8 reacted with Ellman's reagent (at access) and measured immediately, (B) peptides **2-4** (100 µM) at pH 8 incubated at rt for various time-frames and reacted with Ellman's reagent (300 µM).

6 Quantum chemical calculations

6.1 Computational details

All DFT calculations were carried out using the Turbomole 7.4 program. (5) Geometries of all structures were optimized employing the dispersion-corrected BP86 functional [BP86-D3(BJ)] (6–9) and the def2-TZVP (10) basis set (for Pb, this basis set includes the Stuttgart-Dresden effective core potentials) in an implicit solvent with the dielectric constant of ε_r = 80 corresponding to water, employing the COSMO solvation model (11) as implemented in Turbomole 7.4 program. Subsequent vibrational frequency calculations were performed at the same level of theory for all calculated structures *in vacuo* after reoptimization (*in vacuo*). All equilibrium structures possessed zero negative Hessian eigenvalues, so all stationary points were confirmed to be genuine minima on the potential energy surface (PES).

The free energy value corresponding to a particular structure/molecule can be conveniently expressed as (Equation S5):

$$G_S = E_{el} + \Delta G_{solv} + E_{ZPVE} - RTln(q_{trans}q_{rot}q_{vib}) + pV$$

Where E_{el} is the electrostatic potential energy of the molecule *in vacuo* (gas-phase molecular energy), calculated with a slightly larger basis set, def2-TZVPD and the same functional BP86-D3(BJ), ΔG_{solv} is the solvation energy calculated by employing the COSMO-RS method (*vide infra*), E_{ZPVE} is the zero-point vibrational energy whereas $RT\ln(q_{trans}q_{rot}q_{vib})$ are the entropic terms obtained from the rigid-rotor/harmonic oscillator (RRHO) approximation in which a free rotor model was applied for low-lying vibrational modes under 100 cm^{-1} with a smoothing function applied (sometimes denoted as quasi-RRHO, or RRFRHO approximation). The E_{el} and (E_{ZPVE} - $RT\ln(q_{trans}q_{rot}q_{vib})$ + pV) are calculated for the *in vacuo* equilibrium structures. For all structures, we checked that the *in vacuo* minima do not significantly deviate from their solvent counterparts.

The ΔG_{solv} was obtained using Klamt's conductor-like screening model for the realistic solvation method (COSMO-RS). (12) COSMO-RS calculations were carried out using *cosmotherm19* software with the parameter file "BP_TZVPD_FINE_C30_1901.ctd" and the recommended protocol: BP86-D3(BJ)/def2-TZVPD single point calculations *in vacuo* (on top of the *in vacuo* geometries) and in an ideal conductor ($\varepsilon = \infty$) for the solvent geometry, followed by the COSMO-RS (*cosmotherm19*) calculations in the target solvent (water). Throughout, FINE cavities ($cosmo_isorad keyword) were used to increase numerical precision.

6.2 Definition of a complexation energy

The following definition of the complexation Gibbs free energy, $\Delta G_{complexation}$ (which relates to K_d as $\Delta G_{complexation} = RT\ln K_d$), has been used throughout (Equation S6):

$$\Delta G_{complexation} = G_S(products) - G_S(reactants)$$

The "reaction" used is the following (Equation S7):

$$[M(H_2O)_n]^{2+} + (peptide(S^-)_m) \rightarrow [M(peptide(S^-)_m(H_2O)_4]^{c+} + (n-4)H_2O$$

or its alternative (Equation S8):

$$[M(H_2O)_n]^{2+} + (peptide(SH)_m) \rightarrow [M(peptide(S^-)_m(H_2O)_4]^{c+} + mH^+ + (n-4)H_2O$$

Where *M* is the metal ion (Ca(II), Zn(II), and Pb(II)), *n* is the optimal hydration number (6 for Ca(II) and Zn(II), and 5 for Pb(II) - the lone pair on Pb(II) leads to the hemidirected hydration and the *n* = 5 to be the optimal coordination number); (13) *z* denotes the number of released protons (0-4, depending on the particular peptide-metal complex). This approach was previously tested using a similar method that involved calculating structures with deprotonated thiol groups. (14–16) Both led to similar results, which demonstrates the robustness of the computational protocol used.

The global minima of the free peptides in a solvent were obtained using the Maestro/MD-LLMOD program (Schrodinger, Inc.) with default settings. The MD-LLMOD yielded ~150 conformers for each of the four peptides, which were further processed using the above-described QM protocol employed throughout this study to identify the global minimum. This minimum was then used for the calculation of the complexation Gibbs free energy.

7 In vivo studies

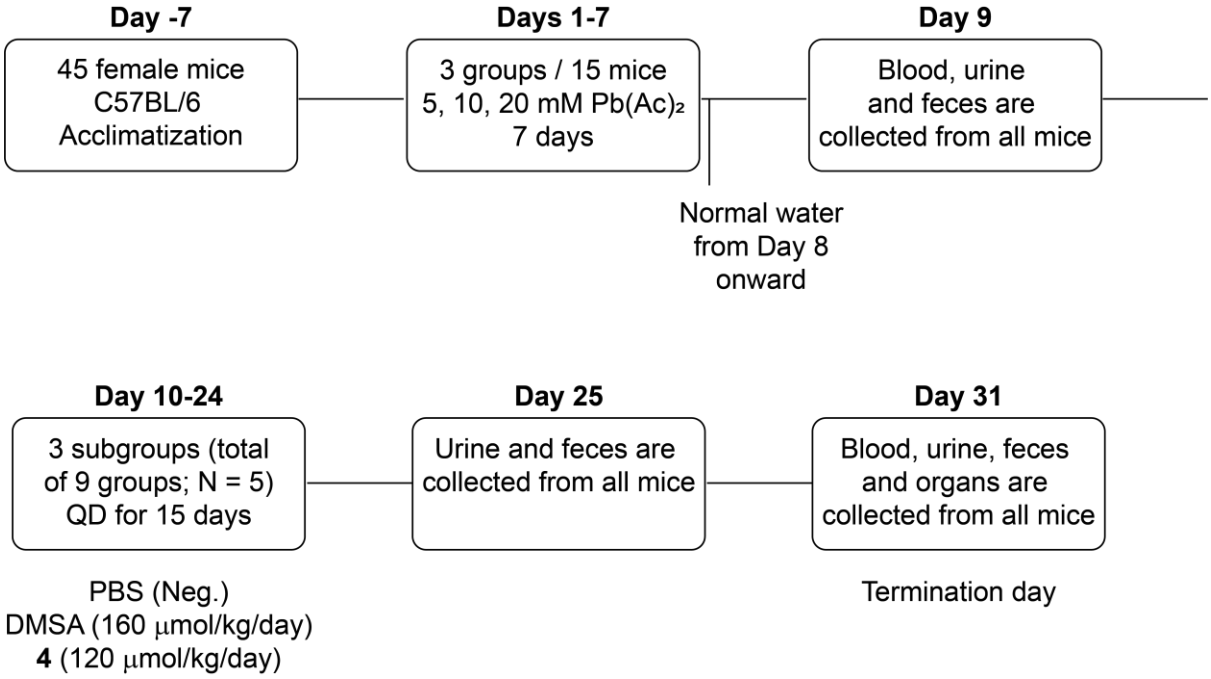

Figure S7 Schematic description of the mouse study reported in this work

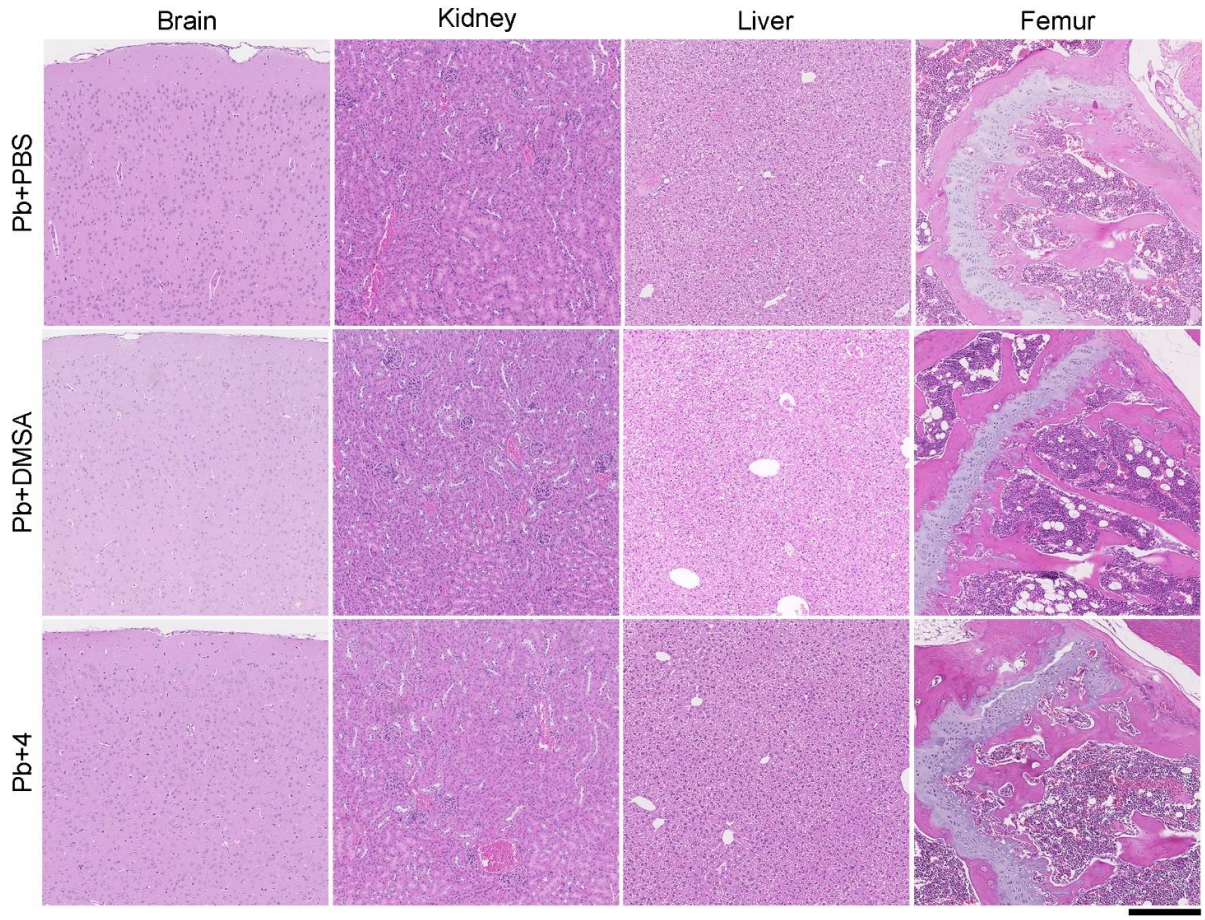

Figure S8 Histopathological pictures of tissues from lead-exposed mice following chelation therapy. Representative photomicrographs of brain, kidney, liver, and femur from mice administered $Pb(Ac)_2$ in drinking water and subsequently treated with PBS (control group), DMSA, or peptide **4** (n=5 per group). All tissues displayed normal morphology across treatment groups. Tissue sections were stained with hematoxylin and eosin. Scale bar = 250 μm.

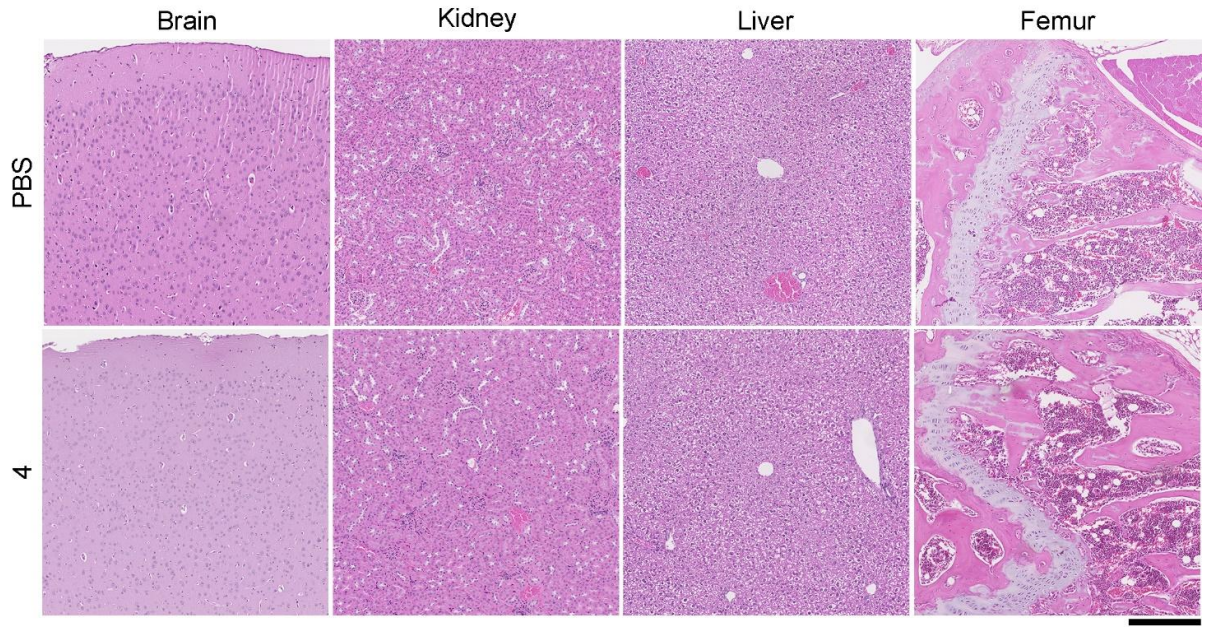

Figure S9 Histopathological pictures of tissues from mice treated with peptide **4** alone**.** Representative photomicrographs of brain, kidney, liver, and femur from mice treated exclusively with peptide **4** (n=5) and PBS control mice (n=4). All tissues exhibit normal morphology. Tissue sections were stained with hematoxylin and eosin. Scale bar = 250 µm.

8 References

1 J. Aaseth, O. Andersen, Chelation Therapy in the Treatment of Metal Intoxication, Elsevier, 2016.

2 M. Feoktistova, P. Geserick, M. Leverkus, *Cold Spring Harb. Protoc.*, 2016, 343–346.

3 Viability assays that are based on reduction, such as MTT, are not suited due to the ability of thiols to reduce the probes.

4 C. K. Riener, G. Kada, H. J. Gruber, *Anal. Bioanal. Chem.,* 2002, **373**, 266–276.

5 S. G. Balasubramani, et al., *J. Chem. Phys.,* 2020, **152**.

6 A. D. Becke, *Phys. Rev. A*, 1988, **38**, 3098.

7 S. H. Vosko, L. Wilk, M. Nusair, *Can. J. Phys.*, 1980, **58**, 1200–1211.

8 J. P. Perdew, *Phys. Rev. B,* 1986, **33**, 8822(R).

9 S. Grimme, *Chem. Eur. J.*, 2012, **18**, 9955–9964.

10 F. Weigend, R. Ahlrichs, *PCCP*, 2005, **7**, 3297–3305.

11 A. Klamt, G. Schüürmann, *J. Chem. Soc. Perkin Trans. 2.*, 1993, 799–805.

12 A. Klamt, *J. Phys. Chem.*, 1995, **99**, 2224–2235.

13 T. Kalvoda, T. Martinek, P. Jungwirth, L. Rulíšek, *J. Chem. Phys.*, 2024, **160**, 084308.

14 T. A. Mohammed, et al., Potent cyclic tetrapeptide for lead detoxification, *Angew Chem. Int. Ed.*, 2021, **60**, 12381–12385.

15 L. Sauser, T. Kalvoda, A. Kavas, L. Rulíšek, M. S. Shoshan, *ChemMedChem*, 2022, **17**.

16 L. Sauser, et al., *Inorg. Chem.*, 2021, **60**, 18620–18624.